9.12 EVALUATION OF CLIMATE-MODEL SIMULATIONS OF HIRS WATER-VAPOUR CHANNEL RADIANCES

Richard P. Allan* and Mark A. Ringer
Hadley Centre for Climate Prediction and Research
Met Office, Bracknell, Berkshire, UK

1. INTRODUCTION

The response of the climate system to an external forcing, such as increasing greenhouse gas concentration, is strongly modulated by feedbacks due to water vapour and cloud, both of which are intrinsically linked to relative humidity. Therefore, it is crucial that relative humidity and its variability are accurately represented in climate models. It is generally believed that the strong positive water vapour feedback predicted by models is robust, and approximates to the feedback experienced for fixed relative humidity (Ingram 2002; Soden *et al.* 2002). However, it has yet to be adequately demonstrated that this approximation applies on decadal timescales to water vapour in the free troposphere (e.g. Sun and Held, 1996). Also, despite the similarity of the clear-sky radiative feedbacks diagnosed from different climate models, it is not clear that their vertical temperature and water vapour changes are consistent (Allan *et al.* 2002). Further, climate models do not agree on the magnitude and sign of cloud feedback (IPCC 2001); observational evidence suggests that decadal changes in temperature lapse rate and cloudiness are not well simulated by current climate models (Gaffen *et al.* 2000; Wielicki *et al.* 2002). Thus, it is crucial that available information on atmospheric temperature and moisture variation is used to test the present-day climate simulated by models.

In the present paper, we evaluate the performance of the Hadley Centre atmospheric climate model (HadAM3) in simulating present-day water vapour and its variability. An important component of the comparison involves the direct simulations of High-resolution Infrared Sounder (HIRS) channel 12 clear-sky radiances, which are primarily sensitive to upper tropospheric relative humidity (UTH). Using the HIRS observational record along with additional satellite data, we attempt to assess the realism of water-vapour distribution and variability in HadAM3. One key question to address is, can the model simulate decadal fluctuations in the HIRS UTH radiances? Also, we assess the effect of differences in spatial and temporal sampling between observations and simulations on the analysis.

* *Corresponding author address:* Richard P. Allan, Hadley Centre for Climate Prediction and Research, Met Office, Bracknell, Berkshire, UK, RG12 2SY. Email: richard.allan@metoffice.com

2. MODEL DESCRIPTION AND SATELLITE DATA

We use HadAM3 (Pope *et al.* 2000) to perform three realisations of the present-day climate forced by observed sea surface temperature and sea-ice over the period 1979-98. To diagnose HIRS channel 12 clear-sky radiances, we use the radiance solver described in Ringer *et al.* (2002). A seasonal ozone climatology is applied and well mixed greenhouse gases are held constant at 1990 levels.

Monthly mean clear-sky brightness temperature data from HIRS Channel 12 (BT_{12}) from 1979-98 is used (Bates *et al.* 2001), along with vertical motion fields from the National Center for Environmental Prediction-National Center for Atmospheric Research 40-year re-analysis (NCEP; Kalney *et al.* 1996). We also employ clear-sky outgoing longwave radiation (OLR) data from the Earth Radiation Budget Satellite (ERBS; Barkstrom *et al*. 1987) over the period 1985-90 and column-integrated water-vapour (CWV) data from the Scanning Multichannel Microwave Radiometer (SMMR; Wentz and Francis 1992) for the period 1979-84 and from the Special Sensor Microwave Imager (SSM/I; Wentz 1997) for 1987-98.

3. CLIMATOLOGY

Figure 1 shows the HadAM3 minus observed climatological fields for DJF and JJA. HadAM3 generally produces lower BT_{12} and clear-sky OLR than the observations. Some of this discrepancy is explained by an overactive South Pacific Convergence Zone in HadAM3, highlighted by a stronger ascent than NCEP over the South Pacific in Fig. 1a and b. More important to the mean bias, however, is the clear-sky sampling difference between infrared observations and model simulations (e.g. Cess and Potter 1987) which will be discussed in section 5. Notably, over dry, subtropical regions, a positive model minus observation difference is present in the BT_{12} comparison. This is likely related to overactive Hadley and Walker circulations in the model. These differences are also present in MAM and SON (not shown) and are most prominent in the Southern Hemisphere, consistent with the circulation errors highlighted in Fig. 1a and b. Column water vapour is underestimated by the model in the tropics and, by a smaller magnitude, overestimated in the extra-tropics compared to the microwave satellite data. Simulated clear-sky OLR is greater than observed values over the Sahara. Table 1 shows the mean HadAM3 minus observation bias over the

oceans to be about –1 K for BT_{12} and about –5 Wm^{-2} for clear-sky OLR for all seasons. Including land points in the analysis (not displayed) does not affect the BT_{12} bias noticeably and slightly reduces the bias for clear-sky OLR. The mean bias in CWV is of variable sign, although this disguises the compensating tropical and extra-tropical differences shown in Fig. 1. RMS bias is approximately 1% of the mean BT_{12}, 2% of the mean clear-sky OLR and 10% of the mean CWV.

Figure 1: HadAM3 minus reanalysis/satellite data for DJF (left) and JJA (right) climatologies: (a,b) HadAM3 minus NCEP 500 hPa vertical motion (mPa s-1) 1979-98; (c,d) HadAM3 minus HIRS BT_{12} (K) 1979-98; (e,f) HadAM3 minus ERBS clear-sky OLR (Wm^{-2}) 1985-89; (g,h) HadAM3 minus combined SMMR and SSM/I record of CWV (kgm^{-2}) 1979-84 and 1988-98. Differences greater than the first positive contour line are coloured. Contour intervals are 2 mPa s^{-1} (vertical motion), 2 K (BT_{12}), 5 W m^{-2} (clear-sky OLR) and 2 kg m^{-2} (CWV); the zero contour line is not plotted. Light blue shading denotes missing data.

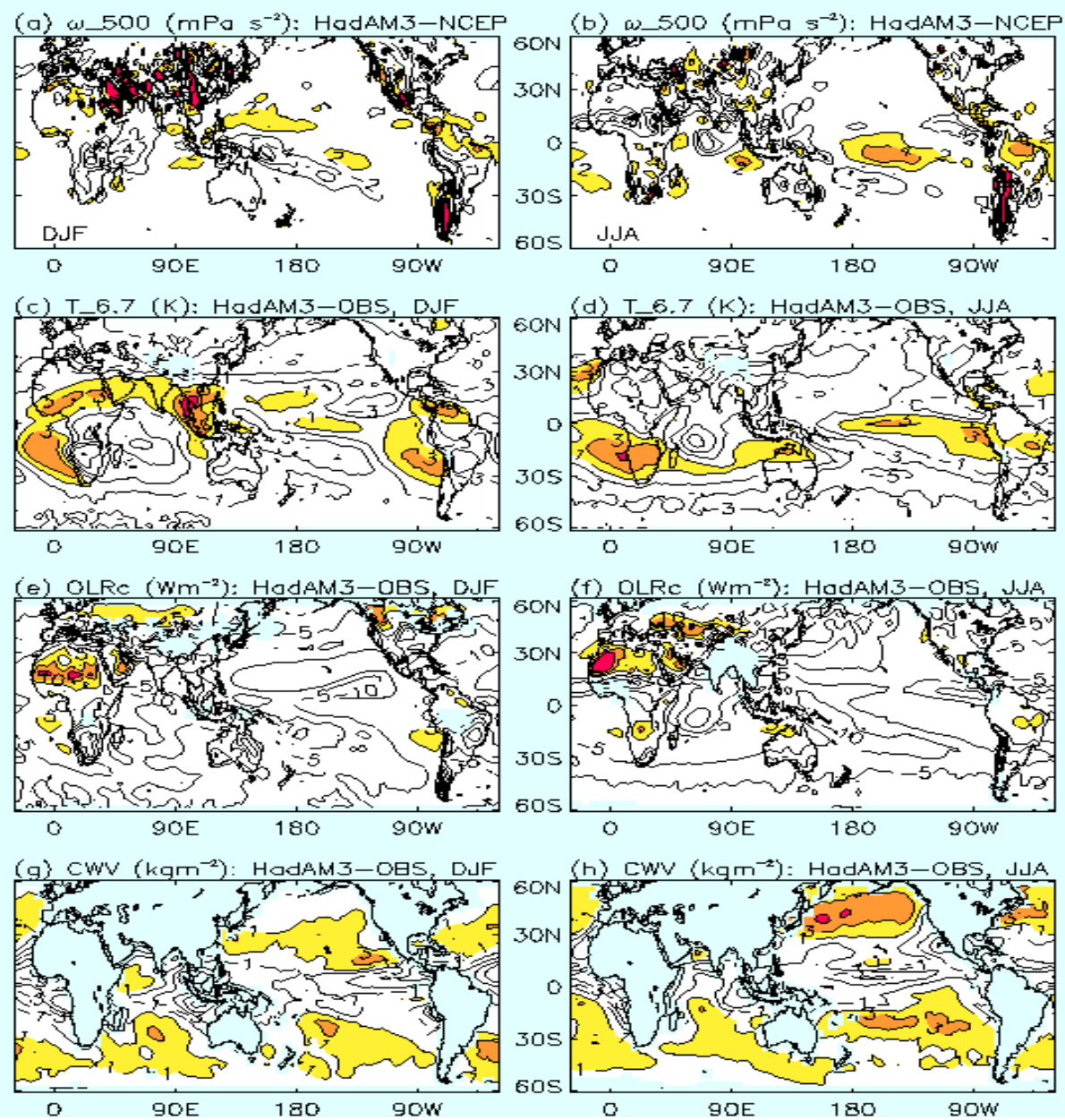

60°S-60°N, ocean		HadAM3	Bias	RMS
BT_{12}(K)	DJF	245.6	-1.2	2.4
	MAM	245.2	-1.2	2.1
	JJA	245.4	-1.3	2.4
	SON	245.6	-1.0	2.4
OLRc	DJF	271.7	-4.9	6.5
(Wm^{-2})	MAM	270.7	-5.1	6.5
	JJA	270.3	-4.9	6.5
	SON	270.8	-4.7	6.5
CWV	DJF	28.4	-0.3	2.7
(kgm^{-2})	MAM	28.9	-0.2	2.5
	JJA	29.0	+0.2	2.2
	SON	28.1	-0.1	2.6

Table 1: 60°S-60°N area-weighted mean BT_{12} (1979-98), OLRc (1985-89) and CWV (1979-84; 1988-98) for HadAM3 climatology and mean and RMS difference with observations over the ocean. Differences are only calculated for each grid point of the climatologies where an observational value is present and subsequently averaged as a mean or root mean squared (RMS) bias.

4. INTERANNUAL VARIABILITY

Many of the differences shown in Figure 1 and Table 1 appear to be systematic. However, it is unclear how these differences affect the climate variability on longer timescales. We now analyse the 1979-98 interannual variability in HadAM3 and the observations. We concentrate our analysis on the tropical oceans because the satellite data coverage is most robust here, and the interannual signal relating to the El Nino Southern Oscillation (ENSO) is largest in these regions. To remove the local dependence of water vapour and radiation on the large-scale circulation, we average over tropical oceans between 30°S and 30°N and remove the mean seasonal cycle.

Figure 2 shows the interannual anomalies of surface temperature, CWV, normalised clear-sky greenhouse effect (g_a, the fraction of surface emission which does not escape as clear-sky OLR) and BT_{12}. Positive anomalies of surface temperature correspond with the warm ENSO events of 1979/80, 1982/3, 1986/7 and 1997/8 that primarily affect DJF. Associated with these warm events are positive CWV anomalies, with HadAM3 reproducing the interannual variability derived from the satellite microwave data. The observed variability for 50 °S and 50°N oceans is

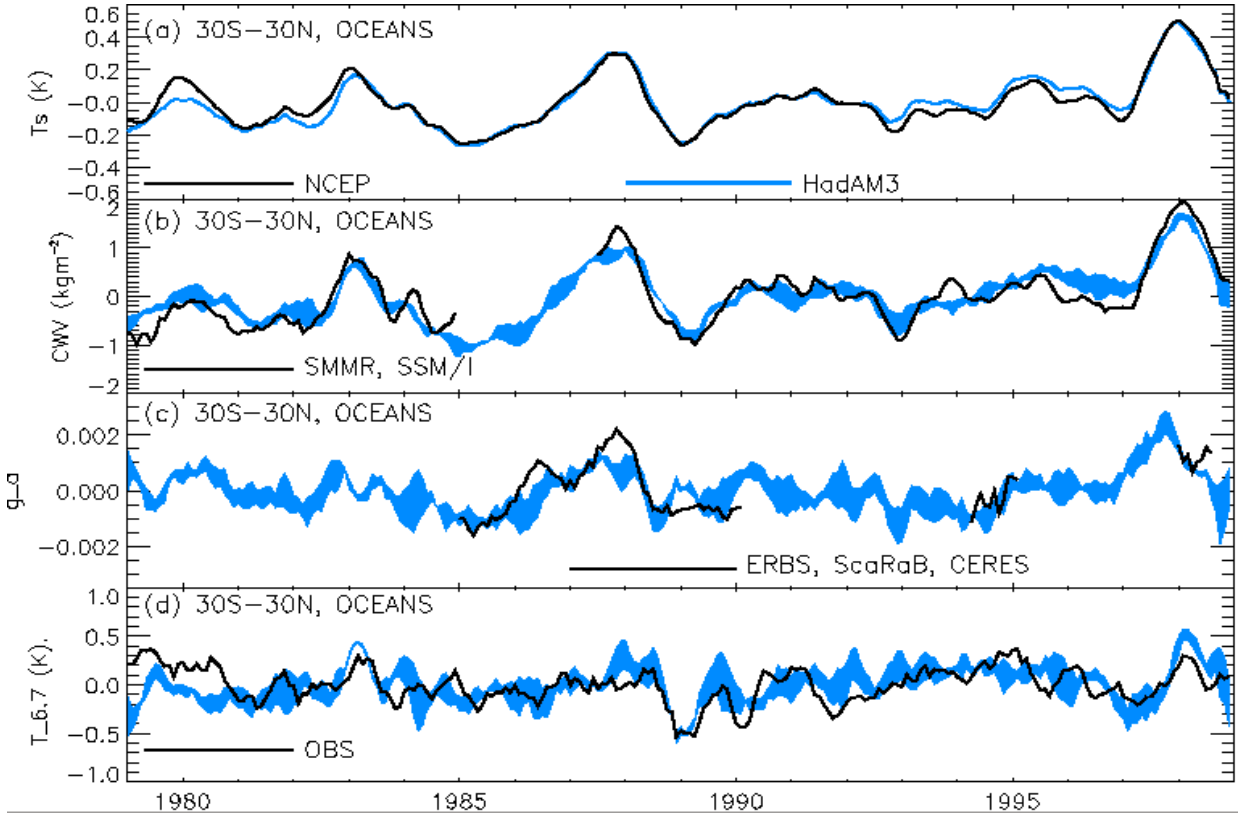

Figure 2: Interannual anomalies over the tropical oceans for (a) surface temperature, (b) column water vapour, (c) normalised greenhouse trapping (fraction of surface emission that does not escape as clear-sky OLR) and (d) HIRS channel 12 brightness temperature. Observations/NCEP are shown in black and the range from a three-member HadAM3 ensemble are shown in blue. The mean monthly climatological values are removed and the time-series smoothed using a five-month moving average.

also well simulated by HadAM3 (not shown). While the agreement is excellent, it is expected that lower tropospheric moisture, which primarily determines CWV, should be well simulated because low level moisture over the tropical oceans are strongly coupled to the sea surface temperature.

Analysing the greenhouse trapping and HIRS channel 12 brightness temperature in Fig. 2c and d provides more information on the accuracy of UTH variability simulated by HadAM3 which is less well understood than lower-level moisture fluctuations. HadAM3 reproduces the observed peak in clear-sky OLR given by ERBS during 1987. However, agreement is less good than that displayed by the GFDL model (Soden 2000). Also shown are the anomalies of g_a (relative to the ERBS climatology) from the Scanner for Radiation Budget (ScaRaB; Kandel *et al.* 1998) in 1994/5 and Clouds and the Earth's Radiant Energy System (CERES; Wielicki *et al*, 1996) in 1998. The observed anomalies are consistent with the simulated variability but provide a rather limited comparison period. Using the entire HIRS record for comparison with the model simulations provides a more comprehensive comparison.

The magnitude of the simulated BT_{12} variability in Figure 2d does not differ markedly to the observations. Peaks during the 1982/3 and 1997/8 ENSO warm events and a minimum during the 1988 cold event are evident in both model and data. It is unclear why a discrepancy appears during 1979/80 in BT_{12}; significant differences in the surface temperature and CWV fields are also evident compared with NCEP and SMMR data respectively.

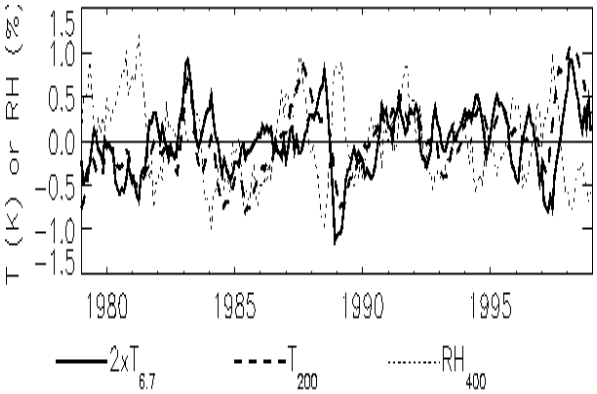

Figure 3: Interannual anomalies of 200 hPa atmospheric temperature (T_{200}), 400 hPa relative humidity (RH_{400}) and 2xBT_{12} (2x$T_{6.7}$) for HadAM3.

While the strong dependence of BT_{12} on UTH has been demonstrated on spatial scales (e.g. Bates *et al*. 2001) it has yet to be established whether this relationship remains robust on interannual timescales. Using the model output, we regress monthly BT_{12} with 200 hPa temperature (T_{200}) and 400 hPa relative humidity (RH_{400}). Although there is an expected strong negative correlation between BT_{12} and RH_{400}, upper tropospheric temperature variations explain an equal portion of the BT_{12} variance as illustrated in Figure 3. The T_{200} curve in Fig. 3 matches the observations and simulations presented in Soden (2000). This suggests that the remaining variability in BT_{12} due to fluctuations in UTH are also adequately simulated by the model.

5. SPATIOTEMPORAL VARIABILITY

We now analyse the spatial nature of the interannual variability of BT12 in the model and satellite data by performing Empirical Orthogonal Function (EOF) analysis on the 20-year monthly time series. The seasonal signal is removed by removing the mean monthly climatology from each data set at each grid point. Figure 4 shows the first EOF pattern for (a) HadAM3, (b) the HIRS satellite observations for 30°S-30°N, and (c) the time-series of (a) and (b).

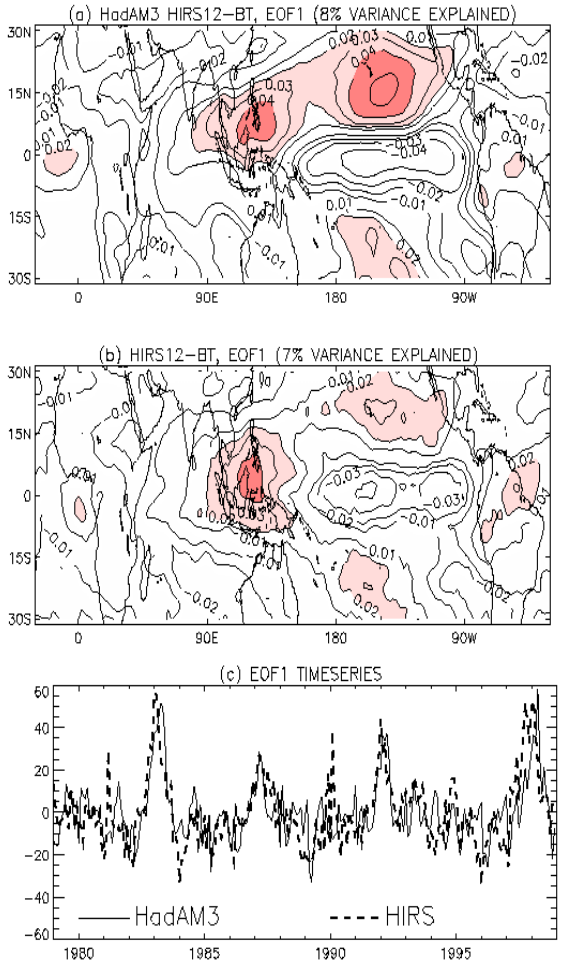

Figure 4: First EOF patterns from interannual monthly anomalies of BT_{12} from (a) HadAM3, (b) HIRS satellite data and (c) the time series of the EOF patterns. Positive anomalies greater than 0.02 are shaded in a and b.

There is excellent agreement between the simulations and the satellite data, with ENSO warm events of 1982/3, 1987/8 and 1997/8 producing higher-than-average BT_{12} over the tropical west Pacific and over the central sub-tropical Pacific. A peak corresponding to the weak 1991/2 ENSO warm event is also captured by the observations and simulations, although this event is not apparent in the surface temperature or CWV variations in Fig. 2 due to the additional effects of the 1991 Pinatubo eruption. Thus the spatial response of UTH, inferred from the BT_{12} relating to the prescribed changes in ocean surface temperature, appears well simulated. However, the model slightly overestimates the magnitude of the signal.

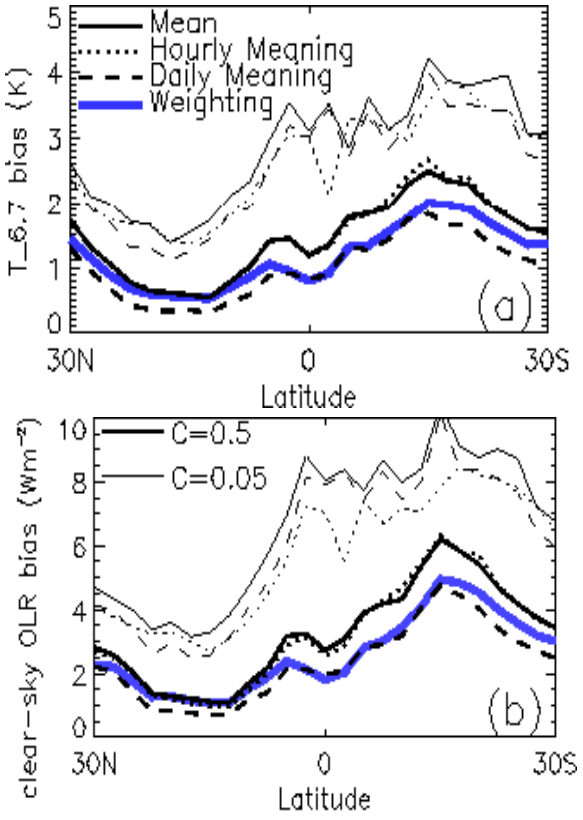

Figure 5: Zonal mean clear-sky (a) BT_{12} and (b) OLR differences for alternative clear-sky sampling scenarios using three hourly clear-sky model diagnostics relative to the standard model output. Thin lines only consider grid-points where cloud fraction (C) is less than 0.5 and thick lines are for C<0.5. Monthly averaging is conducted as a simple average (monthly), by hourly averaging and subsequent averaging of the mean monthly diurnal cycle (hourly) and by averaging daily averages (daily). Also shown are values weighted by clear-sky fraction (blue).

6. EFFECTS OF ADDITIONAL FORCINGS

The effects of additional forcings on the interannual variability were assessed by conducting experiments similar to those presented in the previous sections, but also prescribing the observed changes in greenhouse gases, ozone, solar output and volcanic eruptions. The effect of these forcings is small when considering the interannual variability of CWV and BT_{12}. However, large perturbations are evident in the interannual variations of normalised greenhouse trapping (not shown). This is manifest as large decreases in clear-sky OLR (around -2 Wm^{-2}) following the eruptions of El Chichon (1982) and Pinatubo (1991) and a downward decadal trend in clear-sky OLR due to increased greenhouse gases. Changes in ozone and solar output do not appear to exert a noticeable effect on the diagnostics considered in Fig. 2.

7. SAMPLING ISSUES

In the previous section, we used simulations of satellite radiances to enhance the evaluation of the present-day climate simulated in HadAM3. Despite the consistency in the quantities being compared, there are inconsistencies in the sampling that may affect comparisons. We now assess the sensitivity of the model simulations to the spatial and temporal sampling details.

We conducted additional experiments with HadAM3 in which diagnostics were output every radiation time-step (three hours) for January 1998. Subsequently, the effects of the temporal sampling of the NOAA-14 and NOAA-12 satellites, which carried the HIRS instruments, were assessed by only sampling at each grid point within one hour of the satellite crossing time. The BT_{12} RMS difference between this satellite-sampling method and the standard model sampling is small, representing only around 1% of the model-observation RMS differences over both land and ocean. These findings are consistent with previous work by Engelen *et al.* (2000).

A more important bias is presented by the clear-sky sampling differences between the satellite data and the simulations. The satellite data only samples BT_{12} and clear-sky OLR where there are judged to be enough clear-sky pixels, while the model calculates these clear-sky fields diagnostically at all locations and times by artificially setting cloud amount to zero. Because cloudy regions tend to be more humid than clear regions, the satellite data will effectively be sampling drier, lower-emission regions. A systematic difference of the same sign and magnitude as that expected from the clear-sky sampling bias is evident in the comparisons presented in Fig. 1 and Table 1 for clear-sky OLR and BT_{12}.

Using the radiation time-step diagnostics, we assess the magnitude of this sampling bias by conducting a series of sensitivity tests. Figure 5

shows the clear-sky sampling bias (satellite-like sampling minus model sampling) for (a) BT_{12} and (b) clear-sky OLR. The bias is calculated using clear-sky thresholds of cloud fraction (C) less than 0.05 and 0.5, and for different monthly averaging. The zonal-mean bias is large for clear-sky OLR and BT_{12} compared with the average differences presented in Table 1. Where only grid points with less than 0.05 cloud fraction (C<0.05) were considered, the BT_{12} bias is around 2-3 K. For C<0.5, the bias is about 1-2 K. The clear-sky OLR bias shows similar latitudinal dependence with approximately 2 Wm^{-2} OLR bias corresponding with a 1 K bias in BT_{12}. Weighting clear-sky OLR by cloud fraction provides a similar bias to the C<0.5 case. Using different monthly averaging has little effect on the clear-sky sampling bias.

The results presented here are consistent with previous studies (Cess and Potter 1987; Lanzante and Gahrs 2000) and shows the importance of clear-sky sampling on evaluating systematic biases in simulated longwave radiation fields. It is unlikely that these systematic sampling biases significantly affect the interannual variability. However, we plan to investigate this important issue further.

8. SUMMARY

We present simulations of the present-day climate by forcing the Hadley Centre atmospheric model (HadAM3) with observed sea surface temperature and ice fields. The spatial and temporal variation of moisture and clear-sky radiation produced by the model are evaluated. An important component of the methodology is to directly simulate HIRS channel 12 radiances (and corresponding brightness temperature, BT_{12}) which are sensitive to upper tropospheric humidity. Comparing with the HIRS observations, and additional satellite data of column-integrated water vapour and clear-sky OLR, indicates that HadAM3 can simulate the interannual variability of moisture and clear-sky radiation adequately. The consistent variability of BT_{12} suggests that the model can accurately simulate decadal fluctuations in UTH. However, changes in upper tropospheric temperature also appear to affect the interannual BT_{12} variability. Therefore, the consistent variation of BT_{12} may only signal consistent UTH variation if it can be demonstrated that the model can accurately simulate upper tropospheric temperature. Comparisons from Soden (2000) suggest that that models do a reasonable job at simulating upper tropospheric temperature variation, although analysis from Gaffen *et al.* (2000) suggests models cannot simulate temperature lapse rate variability.

An important limitation to the evaluation of clear-sky longwave diagnostics within climate models is the different spatial and temporal sampling compared to satellite data. We find, by conducting simple sensitivity tests, that the satellite-model clear-sky sampling bias is of the correct sign and magnitude to explain systematic differences between the model and observations over large parts of the globe. Future work will assess whether this effect alters the comparison of the interannual variability.

9. ACKNOWLEDGEMENTS

Thanks to Tony Slingo for making a substantial contribution to the planning and analysis of the HadAM3 simulations and to John Edwards for help with the radiance solver. The work was funded by the Department for Environment, Food and Rural Affairs under contract PECD 7/12/37. ERBS and CERES data were retrieved from the NASA Langley DAAC, the SMMR data from the NASA JPL DAAC, the NCEP reanalysis data from the NOAA-CIRES Climate Diagnostics Center, the SSM/I data from www.ssmi.com/, and the ScaRaB data were provided by the Centre National d'Etudes Spatiales, Toulouse. The HIRS brightness temperature data was kindly supplied by Helen Brindley (the data set was originally provided by J. Bates).

10. REFERENCES

Allan, R. P., V. Ramaswamy, and A. Slingo, 2002: A diagnostic analysis of atmospheric moisture and clear-sky radiative feedback in the Hadley Centre and GFDL climate models, *J. Geophys. Res*., **107**(D17), 4329, doi: 10.1029/2001JD001131**.**

Barkstrom, B. R., E. F. Harrison, R. B. Lee and the ERBE Science Team, 1987: Earth Radiation Budget Experiment (ERBE) archival and April 1985 results, *Bull. Ameri. Met. Soc*., **70**, 1254-1262.

Bates, J. J., D. L. Jackson, F. M. Breon and Z. D. Bergen, 2001: Variability of tropical upper tropospheric humidity 1979-1998, *J. Geophys. Res*., **106**, 32271-32281.

Cess, R. D., and G. L. Potter, 1987: Exploratory studies of cloud radiative forcing with a general circulation model, *Tellus*, **39**, 460-473.

Engelen, R. J., L. D. Fowler, P. J. Gleckler and M. F. Wehner, 2000: Sampling strategies for the comparison of climate model-calculated and satellite-observed brightness temperatures, *J. Geophys. Res.,* **105**, 9393-9406.

Gaffen, D. J., B. D. Santer, J. S. Boyle, J. R. Christy, N. E. Graham and R. J. Ross, 2000: Multidecadal changes in the vertical temperature structure of the tropical troposphere, *Science*, **287**, 1242-1245.

Ingram, W. J., 2002: On the robustness of water vapour feedback : GCM Vertical Resolution and Formulation. *Journal of Climate*, **15**, 917-921.

IPCC, 2001, *Climate Change 2001: The Scientific Basis*, Cambridge University Press, 881 pp.

Kalnay, E. and Co-authors, 1996: The NCEP/NCAR 40-year Reanalysis Project. *Bull. Amer. Meteor. Soc*., **77**, 437-471.

Kandel, R., and Co-authors, 1998: The ScaRaB radiation budget data set, *Bull. Amer. Meteor.*

Soc., **79**, 765-783.
Lanzante, J. R., and G. E. Gahrs, 2000: The 'clear-sky bias' of TOVS upper tropospheric humidity. *J. Climate*, **13**, 4034-4041.
Pope, V. D., M. L. Gallani, P. R. Rowntree and R. A. Stratton, 2000: The impact of new physical parameterisations in the Hadley Centre Climate Model – HadAM3. *Climate Dyn.*, **16**, 123-146.
Ringer, M. A., J. M. Edwards and A. Slingo, 2002: Simulation of satellite-channel radiances in the Met Office Unified Model. *Q. J. R. Meteorol. Soc*., **accepted**.
Soden, B. J., 2000: The sensitivity of the Tropical hydrological cycle to ENSO. *J. Climate*, **13**, 538-549.
Soden, B. J., R. T. Wetherald, G. L. Stenchikov and A. Robock, 2002: Global cooling after the eruption of Mount Pinatubo: a test of climate feedback by water vapour. *Science*, **296**, 727-730.
Sun, D. –Z., and I. M. Held, 1996: A comparison of modelled and observed relationships between interannual variations of water vapour and temperature, *J. Climate*, **9**, 665-675.
Wentz, F. J., 1997: A well calibrated ocean algorithm for SSM/I. *J. Geophys. Res.,* **100**, 7423-7440.
Wentz, F. J., and E. A. Francis, 1992: Nimbus-7 SMMR ocean products, 1979-1984, *Tech Rep. 033192*, 36 pp., Remote Sensing Systems, Santa Rosa, CA.
Wielicki, B. A., B. R. Barkstrom, E. F. Harrison, R. B. Lee, G. L. Smith and J. E. Cooper, 1996: Clouds and the Earth's Radiant Energy System (CERES): an earth observing system experiment. *Bull. Amer. Meteor. Soc*., **77**, 853-868.
Wielicki, B. A., and Co-authors, 2002: Evidence for large decadal variability in the tropical mean radiative energy budget. *Science*, **295**, 841-844.